

# Lawrence Berkeley National Laboratory

## Recent Work

### Title

DIFFUSION AND REACTION STUDIES IN THE ALUMINA-SILICA SYSTEM

### Permalink

<https://escholarship.org/uc/item/2551z6fw>

### Authors

Davis, Robert F.  
Pask, Joseph A.

### Publication Date

1972

ca

DIFFUSION AND REACTION STUDIES IN THE  
ALUMINA-SILICA SYSTEM

Robert F. Davis and Joseph A. Pask  
RECEIVED  
LAWRENCE  
RADIATION LABORATORY

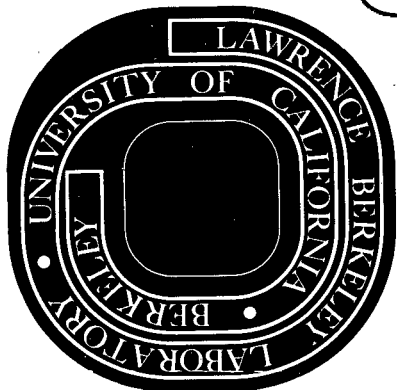
January 1972

LIBRARY AND  
DOCUMENTS SECTION

AEC Contract No. W-7405-eng-48

**TWO-WEEK LOAN COPY**

*This is a Library Circulating Copy  
which may be borrowed for two weeks.  
For a personal retention copy, call  
Tech. Info. Division, Ext. 5545*



ca

## **DISCLAIMER**

This document was prepared as an account of work sponsored by the United States Government. While this document is believed to contain correct information, neither the United States Government nor any agency thereof, nor the Regents of the University of California, nor any of their employees, makes any warranty, express or implied, or assumes any legal responsibility for the accuracy, completeness, or usefulness of any information, apparatus, product, or process disclosed, or represents that its use would not infringe privately owned rights. Reference herein to any specific commercial product, process, or service by its trade name, trademark, manufacturer, or otherwise, does not necessarily constitute or imply its endorsement, recommendation, or favoring by the United States Government or any agency thereof, or the Regents of the University of California. The views and opinions of authors expressed herein do not necessarily state or reflect those of the United States Government or any agency thereof or the Regents of the University of California.

DIFFUSION AND REACTION STUDIES IN THE ALUMINA-SILICA SYSTEM<sup>†</sup>

Robert F. Davis\* and Joseph A. Pask

Inorganic Materials Research Division, Lawrence Berkeley Laboratory  
and Department of Materials Science and Engineering,  
College of Engineering; University of California,  
Berkeley, California 94720

January 1972

ABSTRACT

High-temperature diffusion kinetics and phase relationships between couples of fused silica or cristobalite and sapphire or mullite were investigated in air and helium. Subsolidus liquid formation between sapphire and cristobalite indicates the existence of a metastable system without mullite. A liquid phase is considered to be essential for the nucleation of mullite. The growth rate of mullite exceeded its dissolution rate in semi-infinite fused silica-sapphire couples above 1634°C. The interfacial liquid compositions provided data for a minor revision of the mullite liquidus curve.

Diffusion coefficients calculated from the aluminum profiles vary greatly with concentration and temperature, resulting in a large range of values for apparent activation energy which decrease with increasing Al<sub>2</sub>O<sub>3</sub> content (310 to 60 Kcal/mol for 4 to 22 wt% Al<sub>2</sub>O<sub>3</sub>). The diffusion process in the liquid is considered to be a cooperative movement of oxygen-containing aluminum and silicon complexes whose nature changes

---

<sup>†</sup>Based on a thesis submitted by Robert F. Davis for the Ph.D. degree in ceramic science at the University of California, Berkeley, Calif., Sept. 1970.

\*Now at Corning Research Center, Corning, New York.

with composition and temperature; this change in the diffusing species contributes to the range in values of experimental apparent activation energies.

## I. Introduction

Studies of ionic self-diffusion and interdiffusion in glasses, and of the interdiffusion and dissolution processes which occur between refractory oxides and glasses have been receiving increased attention as shown by the reviews of Williams<sup>1</sup> and Doremus.<sup>2</sup> Paladino and Kingery<sup>3</sup> and Oishi and Kingery<sup>4</sup> have studied the self-diffusion of aluminum and oxygen, respectively, in  $\text{Al}_2\text{O}_3$  while a number of investigators have determined the oxygen diffusion in vitreous silica<sup>5-8</sup> and the dissolution of sapphire in silicate melts.<sup>9</sup> A dearth of information exists, however, concerning interdiffusion and dissolution in the  $\text{Al}_2\text{O}_3$ - $\text{SiO}_2$  system.

A phenomenological approach was undertaken by de Keyser<sup>10</sup> in studies of reactions between pellets of polycrystalline alumina and cristobalite at  $1600^\circ\text{C}$  for 2 h. He found that a liquid phase formed surrounding the cristobalite grains and that penetration of a  $\text{SiO}_2$ -rich liquid into the  $\text{Al}_2\text{O}_3$  pellet initiated the formation of mullite crystals.

Staley and Brindley<sup>11</sup> have also conducted subsolidus reaction experiments at  $1500$  and  $1550^\circ\text{C}$  using pressed pellets of  $\text{SiO}_2$  (cristobalite) in contact with single crystals or pressed pellets of  $\text{Al}_2\text{O}_3$ , as well as mixed powders. They concluded that the formation of an amorphous phase was an essential feature of the reaction. No mullite was observed when the polycrystalline  $\text{Al}_2\text{O}_3$  pellet was replaced by sapphire. Wahl et al.<sup>12</sup> reported a reaction with powder mixtures of cristobalite and corundum at temperatures as low as  $1200^\circ\text{C}$  which showed no mullite.

The objectives of this study were to determine the nature of the dissolution of alumina by silica, to describe the kinetics of dissolution, and to relate the latter to possible operative mechanisms.

## II. Experimental Procedure

### (1) Sample Preparation and Experimentation

Diffusion couples were prepared using 11/32 in. dia. by 1/16 in. single crystals of alumina (sapphire)\* or mullite<sup>†</sup> and fused silica,<sup>‡</sup> cristobalite,<sup>§</sup> or 15 wt% Al<sub>2</sub>O<sub>3</sub>-85 wt% SiO<sub>2</sub>.<sup>§†</sup> These materials were cut into appropriate sizes, polished to optical smoothness, and checked for flatness against their couple counterpart to effect good bonding and prohibit the entrapment of He or air in an irregular surface. Each component was washed in ethyl alcohol and placed into 11/32 in. dia. by 5/16 in. spun molybdenum or Coors CN-2, 99.8% alumina crucibles. Four to six couples containing the different phases were annealed simultaneously. In each couple the silica phase or glass rested upon the sapphire or mullite.

\*Union Carbide, Torrance, Calif. Spectrographic analysis: Si 0.21, Na 0.05, B 0.005, Sn 0.005, Fe 0.004, Ca 0.001, Ti 0.001 wt% of oxide.

†Carborundum Corp., Niagara Falls, N.Y. Spectrographic analysis by American Spectrographic Labs., San Francisco, Calif.: as oxides-- Ca 0.006, Fe 0.02, Na 0.12, Mg 0.01, Zr 0.01, Ti 0.005, Cr 0.003, Mn <0.001 and Cu <0.005, Al and Si (principal constituents). Electron microprobe analysis showed an average of 75.8 wt% Al<sub>2</sub>O<sub>3</sub> (variance ± 1 wt%). Stoichiometric mullite (3Al<sub>2</sub>O<sub>3</sub>·2SiO<sub>2</sub>) contains 71.8 wt% Al<sub>2</sub>O<sub>3</sub>; 2:1 mullite, 77.3 wt% Al<sub>2</sub>O<sub>3</sub>.

‡Amersil (Div. of Englehard Ind. Inc., Hillside, N.J.). Spectrographic analysis: Al 0.045, Fe 0.015, Ca 0.0005 wt% of oxide.

§Ga. Inst. of Tech. Exp. Station, Atlanta, Ga. (prepared by crystallization of fused silica rod). Spectrographic analysis: Al 0.23, Fe 0.092, Na 0.08, Ti 0.028, Ca 0.02, B 0.01, Mg 0.008 wt% of oxide.

§Prepared from intimately mixed -325 Corning 7940 fused silica and Alcoa XA-16 reactive alumina dried at 110°C, vacuum melted at 1800°C for 30 min. in molybdenum containers, and quenched in flowing He.

†All subsequent compositions will be given in wt% unless specified otherwise.

The molybdenum crucibles were covered by a 1-1/8 in. I.D. molybdenum crucible to equalize heat distribution and to reduce silica vaporization, and positioned in the center of a 4 in. dia. by 8 in. tantalum (Ta) resistance heating element of a model 466S-4 Brew furnace. This arrangement was modified for all temperatures below 1650°C by placing the diffusion couples, topped by 1000 gram platinum weights, into 7/8 in. I.D. Al<sub>2</sub>O<sub>3</sub> crucibles.

The Ta chamber was heated to 1200°C for 1 h at 10<sup>-6</sup> torr to remove any organic and hydroxide films from the sapphire surfaces.<sup>13,14</sup> It was then isolated and high purity He\* allowed to slowly enter until atmospheric pressure was attained. The temperature was rapidly raised to the working point to avoid reaction at lower temperatures and subsequent cracking of the sapphire due to its difference in thermal expansion from that of fused silica.

The principal temperature range in the static He atmosphere was 1650° to 1800°C in 50° intervals for different times depending on the temperature (Table I). Mullite-silica couples fired in He above 1650°C could not be analyzed due to a reaction involving residual silica-rich glass and silicon impurities in the mullite which resulted in the entrapment of vapor species as bubbles at the interface.<sup>15</sup> Couples of sapphire-cristobalite were also heated at 1550° and 1580°C.

The temperature of the specimens heated in He was measured by a W-5 Re/W-26 Re thermocouple (accuracy ± 7° at 1800°C) connected to a Leeds and Northrup Speedomax H Recorder-Controller and cross-checked with a Leeds and Northrup optical pyrometer utilizing black-body conditions.

\*Analysis showed 2 ppm N<sub>2</sub> and 1 ppm O<sub>2</sub>.



For the air anneals,  $\text{Al}_2\text{O}_3$  crucibles were placed in a Kanthal Super 33 element furnace preheated to  $1200^\circ\text{C}$ , and a heating schedule utilized similar to that for the He runs. With these elements,  $1650^\circ\text{C}$  was the highest temperature that could be maintained for a long period of time. The temperature was measured by a Pt-6 Rh/Pt-30 Rh thermocouple (accuracy  $\pm 5^\circ$  at  $1650^\circ\text{C}$ ) and monitored by a Leeds and Northrup Speedomax H recorder.

A very slow (48-96 h) and carefully controlled cooling rate was employed for all runs to avoid the loss of integrity at the interface due to the difference in thermal expansion. The specimens were subsequently mounted in polyester resin, sectioned in half parallel to the direction of diffusion, and remounted for polishing.\*

## (2) Electron Microprobe Analysis

The Al concentration versus distance profiles were determined from the highly polished carbon-coated specimen surfaces using a Materials Analysis Co. Model 400 electron microprobe set at a beam potential of 15 KV and a sample current of  $0.025 \mu$  amps. The electronic data was automatically recorded on computer cards for further correction and evaluation.

Crystallization of mullite occurred in the diffusion zone on cooling from temperatures above  $1650^\circ\text{C}$  resulting in very irregular diffusion profiles when determined with a  $1 \mu$  point beam. To surmount this difficulty, the beam was tuned so that it very rapidly scanned a line  $100 \mu$

---

\*Polishing consisted of 2 min each on a  $240 \mu$  and  $15 \mu$  metal bonded diamond lap, 24 h each on a  $6 \mu$  and  $1 \mu$  diamond lap, and 6 h in a syntron vibrated Linde A ( $0.03 \mu \text{Al}_2\text{O}_3$ ) water slurry.

long in a direction parallel to the interface of the couple. Following ten seconds of counting, the data was recorded, and the scanning beam automatically moved  $1 \mu$  toward the interface. It should be noted that while the measured X-ray intensity decreased as the beam deviated from the center of the cross hairs, it did not cause inaccuracies in the concentration data, as the  $\text{Al}_2\text{O}_3$  and  $\text{SiO}_2$  standards were measured in the same manner.

### III. Results and Discussion

#### (1) Diffusion Profiles and Phase Equilibria

The experimental conditions and a portion of the resulting diffusion data are presented in Table I. Typical Al concentration versus distance profiles obtained at  $1650^\circ$  and  $1800^\circ\text{C}$  are shown in Fig. 1. No diffusion of silica into the sapphire was detected in any experiment. The interfacial concentrations remained constant with time at a temperature and were the same for the mullite-fused silica couples annealed at an equivalent temperature. This condition indicates that diffusion in the liquid, not the reaction at the interface, is the rate controlling step. These interfacial concentrations thus correspond to equilibrium liquid compositions in contact with mullite. The resulting liquidus curve is shown in Fig. 2 superimposed on the diagram after Aramaki and Roy.<sup>16</sup>

#### (2) Microstructure

A representative cross-section of the cristobalite-sapphire couples annealed at  $1550^\circ$  and  $1580^\circ\text{C}$  is shown in Fig. 3 for the conditions of  $1580^\circ\text{C}$ , 8 days. Of substantial interest is the visible absence of the mullite phase at these temperatures, and the appearance of an amorphous phase whose composition at the interface lies on the extended mullite

liquidus curve (Fig. 2). The diffusion profiles of Al extend 5-10  $\mu$  into the zones containing cristobalite. This microstructure thus raises the question of the actual existence of the expected equilibrium mullite phase at the interface at these temperatures.

From a theoretical viewpoint, Kidson<sup>17</sup> shows that the application of Fick's first law to diffusion in binary systems in which occurs a single intermediate solid solution phase leads to an expression of the form

$$W_{\beta} = B_{\beta} \sqrt{t} \quad (1)$$

where  $W_{\beta}$  is the width of the intermediate phase  $\beta$  as a function of time ( $t$ ). The two end phases,  $\alpha$  and  $\gamma$ , contain higher and lower interfacial concentrations, respectively, of the diffusing species than does the  $\beta$  phase. Kidson argues that the complete absence of the  $\beta$  phase with the interfacial concentrations of the  $\alpha$  and  $\gamma$  phases unchanged must be rejected on thermodynamic grounds, as it would then imply a discontinuity in the chemical potential at the resulting  $\alpha$ - $\gamma$  interface. This would be a contradiction of the requirement that the chemical potential be continuous and monotonic throughout the specimen cross-section.

The appearance of an amorphous phase in the cristobalite-sapphire couples at subsolidus temperatures precludes such a discontinuity and leads to the conclusion that its occurrence is energetically more favorable and that its formation is a precursor to its immediate reaction with alumina to nucleate the equilibrium mullite phase. This phenomenon of initial formation of a nonequilibrium liquid would necessitate a metastable phase diagram without the mullite phase (Fig. 4) in which

the liquidus curves originating from pure  $\text{Al}_2\text{O}_3$  and  $\text{SiO}_2$  would be extended to lower temperatures.\* A somewhat analogous diagram has been shown by Kingery<sup>19</sup> for the  $\text{K}_2\text{O}\cdot 2\text{SiO}_2$ - $\text{SiO}_2$  system in which the equilibrium  $\text{K}_2\text{O}\cdot 4\text{SiO}_2$  phase crystallizes very slowly from a cooled melt.

The initial step in the diffusion process (e.g.  $1500^\circ\text{C}$ ) would then be for the formation of a liquid film at the interface having a composition range from  $\rho$  to  $\rho'$ , as shown in Fig. 4. The alumina-rich liquid,  $\rho'$ , reacts immediately with the sapphire surface to nucleate mullite and to form liquid  $\rho''$ . The system then reverts to the phase diagram for fused silica-sapphire showing mullite with the remaining liquid reducing its  $\text{Al}_2\text{O}_3$  content through diffusion into (and subsequent dissolution of) the cristobalite compact.

The failure of the nucleated mullite to grow to an observable thickness at the lower temperatures is attributed to a growth rate slower than its dissolution rate into the silica liquid. Staley and Brindley<sup>11</sup> showed that, at the temperatures they employed, mullite growth did not occur until the liquid phase became saturated with alumina. If all the mullite formed at the interface is dissolved, the reaction sequence of solution of alumina, and the nucleation and dissolution of mullite may be repeated continuously until the entire silica phase begins to be saturated with  $\text{Al}_2\text{O}_3$ .

---

\*It should be noted that a simple binary metastable phase diagram with a eutectic temperature below that for  $\text{SiO}_2$ -mullite could also be realized by an extension of the  $\text{SiO}_2$ -liquidus and  $\text{Al}_2\text{O}_3$ -liquidus curves shown in the phase diagram reported by Bowen and Grieg.<sup>18</sup>

Figure 5 shows the microstructures of the cross-sections of fused silica-sapphire couples annealed at 1650°, 1700°, 1750° and 1800°C as observed at room temperature. At 1650°C the diffusion zone is primarily an amorphous phase. As before, the aluminum profile extends 5-10  $\mu$  into the cristobalite formed by devitrification at the annealing temperature. An important feature is the small but discernable appearance of a mullite layer at the sapphire interface dictating that at this temperature its rate of growth has surpassed its solution rate in the liquid phase.

The micrographs of the couples run at 1700°, 1750° and 1800°C reveal mullite needles which crystallized in the diffusion zone on cooling due to the resulting  $\text{Al}_2\text{O}_3$  saturation. They also show that the growth rate of the separate interfacial mullite grown at test temperature has increased and that the fused silica has retained its amorphous state. The composition of the precipitated mullite was determined by point beam microprobe analysis to be ~74%  $\text{Al}_2\text{O}_3$ . Since mullite crystallized from a stoichiometric 3:2 mullite melt<sup>16</sup> contains 77.4%  $\text{Al}_2\text{O}_3$  ( $2\text{Al}_2\text{O}_3 \cdot \text{SiO}_2$ ), it is suggested that the lower  $\text{Al}_2\text{O}_3$  contents of the diffusion zones are responsible for the lower  $\text{Al}_2\text{O}_3$  concentration of the needles.

The solid solution range of the interfacial 3:2 mullite was determined from a 15%  $\text{Al}_2\text{O}_3$  glass-sapphire couple annealed at 1700°C for 11 days. This allowed the mullite layer to grow to a greater thickness since the silica was already essentially saturated with  $\text{Al}_2\text{O}_3$  and dissolution did not occur. The values, averages of a number of profiles extrapolated to the interfaces, ranged from 70.5%  $\text{Al}_2\text{O}_3$  at the liquid boundary to 73.5% at the sapphire interface. This range is in agreement within experimental error, with the limits of 71.8-74.3%  $\text{Al}_2\text{O}_3$  determined

by Aramaki and Roy<sup>16</sup> for 3:2 mullite.

To determine the temperature at which the interfacial mullite would cease to be recognized by optical methods in semi-infinite fused silica-sapphire couples, values from Table I of mullite thickness versus the square root of time were plotted for the 1650°, 1700°, and 1750°C runs as shown in Fig. 6. Thickness values for a number of constant times were taken from this graph, plotted versus temperature and extrapolated to zero thickness (Fig. 7). This procedure revealed that mullite under these conditions would cease to grow to an observable thickness at temperatures below 1634°C.

Also, thickness values for 4, 6 and 8 h were determined as above, plotted versus temperature in Fig. 7, and extended to 1800°C. The amounts of growth of interfacial mullite that should appear at this temperature after these times were 1.9, 2.3 and 2.6  $\mu\text{m}$  respectively. These small values, coupled with the extensive crystallization of mullite in the diffusion zone on cooling, explain the difficulty in discerning a distinct interfacial layer of mullite for these relatively short times at 1800°C (Fig. 5).

### (3) Diffusion Calculation Methods

The bases for all diffusion theories are Fick's first and second laws.<sup>20-22</sup> The units generally employed are centimeters and seconds with concentration being expressed per unit volume. If there is a significant change in the density of the solvent with the introduction of the solute atoms, as occurs when  $\text{Al}_2\text{O}_3$  diffuses into  $\text{SiO}_2$ , this change must be accounted for in the calculation of the chemical interdiffusion coefficient,  $\tilde{D}$ .

Density determinations were made by the liquid displacement technique on glasses containing 5-40%  $\text{Al}_2\text{O}_3$  in 5% intervals, which were prepared using the procedure indicated for the 15%  $\text{Al}_2\text{O}_3$  glass. Pure ethyl alcohol was selected as the displacement medium, and an account made for the change in its density with temperature. The composition of the glasses was analyzed with the microprobe and found to be within one percent of the initial batch value. The resulting graph of density versus wt%  $\text{Al}_2\text{O}_3$  is shown in Fig. 8. As a point of interest, a curve calculated from the data of Huggins and Sun<sup>23</sup> for quickly cooled glasses of the same composition is also shown.

Frazier, et al.<sup>24</sup> have written computer programs which correct the raw microprobe data for dead time, drift, background, absorption, and fluorescence and record the composition of each data point in weight percent of the elements or their oxides. Incorporation of additional programs containing the above density relationship served to determine and plot the profiles of concentration (g/cc) of Al versus distance (Fig. 1).

The extent of the growth of the mullite solid solutions at the interfaces in the sapphire-silica diffusion couples was too small for the times employed to obtain a reliable concentration profile through the mullite. Thus only the chemical diffusivity of Al in  $\text{SiO}_2$  was determined in this study. A Boltzmann-Matano analysis<sup>25,26</sup> was used for this operation as  $\bar{D}$  was found to vary as a function of the concentration of Al.

#### (4) Diffusion Data

A fundamental assumption in the derivation and use of the Boltzmann-Matano analysis is that the process is diffusion controlled. This was

evidenced by the linearity of the plots of the penetration distance from the Matano interface for a given concentration as a function of the square root of time.

The Matano interface and  $\tilde{D}$  were determined by taking the concentration-distance coordinates directly from the smoothed Cal-Comp plots (e.g. Fig. 1) and inserting them into computer programs written by Appel.<sup>27</sup> The values of  $\tilde{D}$  were found to vary exponentially (correlation coefficient range 0.84-0.94) with the aluminum ion concentration ranging over approximately three orders of magnitude for each temperature as shown by the least squares determined plot of Fig. 9 for 1800°C. The graphs and the equations which describe them (Table I) are representative for all times at a particular temperature.  $\tilde{D}$  values were determined from each of these equations for several values of concentration and plotted against  $1/T$  °K (Fig. 10). A least squares analysis whenever applicable resulted in an Arrhenius equation consistent with the form  $\tilde{D} = D_0 \exp(-Q/RT)$  for the temperature dependence of  $\tilde{D}$  for each concentration as presented in Table II. The activation energies for the higher concentrations were evaluated on the basis of only two or three temperatures, as these compositions do not exist in the lower temperature diffusion profiles.

The results show that the activation energy and the pre-exponential ( $D_0$ ) values are extremely high at the low aluminum concentrations, but decrease as the concentration increases. The wide range of values suggests that the diffusion mechanism is complex and that the structure of the liquid glass and the nature of the diffusing species are changing.



These phenomena must be dependent upon the nature of the coordination of the  $\text{Al}^{+3}$  ion within the silica structure at different  $\text{Al}_2\text{O}_3$  concentrations and temperatures. In studies on  $\text{Na}_2\text{O}-\text{Al}_2\text{O}_3-\text{SiO}_2$  glasses, tetrahedral (both of the tricluster and network-forming types) and octahedral coordination of  $\text{Al}^{+3}$  have been proposed under certain conditions.<sup>28-31</sup> McDowell and Beal<sup>32</sup> have shown that  $\text{Al}_2\text{O}_3-\text{SiO}_2$  glasses containing 5 mol% (8.2 wt%)  $\text{Al}_2\text{O}_3$  or less did not exhibit phase separation on slow cooling; however, the 10 mol% (15.9 wt%) glasses showed separation even when rapidly quenched. This difference is considered to be associated with an average increase in the  $\text{Al}^{+3}$  coordination either at temperature or on cooling as the  $\text{Al}_2\text{O}_3$  is increased. Extrapolation of the viscosity data of Rossin et al. to the temperatures employed by the present authors provides additional indications of changes in the liquid structure of aluminum silicates; approximately a six-order decrease in viscosity and a decrease of activation energy from 120 to 50 kcal/mole was realized with an increase from zero to 63 wt% of  $\text{Al}_2\text{O}_3$ .<sup>33</sup>

Complex diffusing species have been proposed to explain diffusion data in ternary silicate liquids. King and Koros<sup>34</sup> and Towers and Chipman,<sup>35</sup> using a 20  $\text{Al}_2\text{O}_3 \cdot 40 \text{CaO} \cdot 40 \text{SiO}_2$  liquid at 1350° to 1520°C, found a higher value for the activation energy for  $\text{Ca}^{+2}$  diffusion than that which would be expected for conduction.<sup>36</sup> This suggests that cation-anion groups are important contributors to diffusion. Reed and Barrett<sup>37</sup> have also demonstrated that under an actual Ca, Si and O concentration gradient in this liquid, the diffusion rate of oxygen is controlled by the calcium migration rate.

Coupling these findings with the diffusion and viscosity data, the conclusion is reached that diffusion in the binary  $\text{Al}_2\text{O}_3$ - $\text{SiO}_2$  glasses is a cooperative movement of oxygen-containing aluminum and silicon complexes. As mullite (or  $\text{Al}_2\text{O}_3$ ) enters the fused silica structure, the oxygens must adjust to form the glass configuration--an entity which is in a state of continual change. With the movement of the Al complex along the concentration gradient, there is a corresponding flux of a Si complex toward the interface. These complementary movements can be visualized as viscous molecular masses of varying size moving by a cooperative rotation mechanism in which a minimum number of bonds must be broken. It is expected that the complexes which effect the diffusion through the glass become progressively smaller with addition of  $\text{Al}_2\text{O}_3$  and increase of temperature. With a change in the structure of the glass, the diffusing complexes would also be expected to change. A detailed interpretation of dissolution behavior on the basis of activation energy values then becomes rather ineffective.

#### IV. Conclusions

(1) Mullite is easily nucleated at fused silica-sapphire interfaces. Its growth rate, however, is surpassed by its dissolution rate below  $1634^\circ\text{C}$  in semi-infinite diffusion couples. This temperature is expected to be lower if the dissolution rate, which is dependent upon the degree of saturation of fused silica with  $\text{Al}_2\text{O}_3$ , is reduced.

(2) The interfacial compositions of fused silica-mullite or fused silica-sapphire couples below  $1800^\circ\text{C}$  describe a revised mullite-silica liquidus curve.

(3) Nucleation of mullite at cristobalite-sapphire interfaces at temperatures below the cristobalite-mullite eutectic (and possibly above the eutectic temperature) by solid state reaction is difficult; an amorphous phase forms first which indicates the existence of a metastable phase diagram with no mullite phase. The liquid immediately reacts with sapphire to nucleate mullite and to form a liquid of constant composition at the interface which is in equilibrium with mullite.

(4) The solid solution range of the mullite grown at 1750°C extends from 70.5 to 73.5%  $\text{Al}_2\text{O}_3$  and is nominally  $3\text{Al}_2\text{O}_3 \cdot 2\text{SiO}_2$ . Needle-like mullite precipitated from aluminum silicate liquids on cooling is nominally  $2\text{Al}_2\text{O}_3 \cdot \text{SiO}_2$ .

(5) The mechanism of diffusion involves a diffusion-controlled cooperative movement of complex aluminum-oxygen and silicon-oxygen species whose size and structure is dependent on temperature and the  $\text{Al}_2\text{O}_3$  concentration. The varying size of the diffusing species and the change in glass structure affect the diffusivity and are responsible for the extremely large range of apparent activation energy values.

#### Acknowledgments

Grateful appreciation is extended to George Georgakopoulos for guidance in the use of the electron microprobe, George Dahl for polishing the many samples, and Marvin Appel, Tom Seward III and İlhan Aksay for their valuable discussions. This work was supported by the Edward Orton Jr. Ceramic Foundation and the United States Atomic Energy Commission.

## References

1. E. L. Williams, "Diffusion in Glass: I," Glass Industry 43 [3] 113-17 (1962); "II," ibid, [4] 186-91; "III," ibid, [5] 257-61; "IV," ibid, [7] 394-95, 402; "Appendix," ibid, [8] 437-40.
2. R. H. Doremus, pp. 1-71 in Modern Aspects of the Vitreous State, Vol. II, Edited by J. D. Mackenzie, Butterworth & Co. Ltd., London, 1962.
3. A. E. Paladino and W. D. Kingery, "Aluminum Ion Diffusion in Aluminum Oxide," J. of Chem. Phys., 37 [5] 957-62 (1962).
4. Y. Oishi and W. D. Kingery, "Self-Diffusion of Oxygen in Single Crystal and Polycrystalline Aluminum Oxide," J. of Chem. Phys., 33 [2] 480-86 (1960).
5. F. J. Norton, "Permeation of Gaseous Oxygen through Vitreous Silica," Nature (London) 171 [4789] 701 (1961).
6. E. W. Suvov, "Diffusion of Oxygen in Vitreous Silica," J. Am. Ceram. Soc., 46 [1] 14-20 (1963).
7. E. L. Williams, "Diffusion of Oxygen in Fused Silica," J. Am. Ceram. Soc., 48 [4] 190-94 (1965).
8. W. N. Lawless and B. Wedding, "Photometric Study of the Oxygen Diffusivity in an Aluminosilicate Glass," J. of Applied Physics, 41 [5] 1926-29 (1970).
9. A. R. Cooper, Jr., W. D. Kingery, Y. Oishi and B. N. Samaddar, "Dissolution in Ceramic Systems: I, Molecular Diffusion, Natural Convection, and Forced Convection Studies of Sapphire Dissolution in Calcium Aluminum Silicate," J. Am. Ceram. Soc., 47 [1] 37-43 (1964); "II, Dissolution of Alumina, Mullite, Anorthite, and Silica

- in a Calcium-Aluminum Silicate Slag," *ibid.*, [5] 249-54; "III," Boundary Layer Concentration Gradients," *ibid.*, 48 [2] 88-95 (1965).
10. W. L. DeKeyser, pp. 243-57 in *Science of Ceramics*, Vol. II, Edited by G. H. Stewart, Academic Press, New York, 1963.
  11. W. G. Staley, Jr. and G. W. Brindley, "Development of Noncrystalline Material in Subsolidus Reactions Between Silica and Alumina," *J. Am. Ceram. Soc.*, 52 [11] 616-19 (1969).
  12. F. M. Wahl, R. E. Grim, and R. B. Graf, "Phase Transformations in Silica-Alumina Mixtures as Examined by Continuous X-ray Diffraction," *Am. Mineralogist*, 46 [5] 1064-76 (1961).
  13. G. A. Parks, "The Composition and Reaction Capability of Oxide Surfaces," *Research in Mineral Proc.*, Prog. Rept. 65-1, Stanford Univ. June 1965.
  14. M. Robinson, J. A. Pask, D. W. Fuerstenau, "Surface Charge of Alumina and Magnesia in Aqueous Media," *J. Am. Ceram. Soc.*, 47 [10] 516-20 (1964).
  15. R. F. Davis, I. A. Aksay, and J. A. Pask, "Decomposition of Mullite," *J. Am. Ceram. Soc.*, 55 [2] (1972).
  16. S. Aramaki and R. Roy, "Revised Phase Diagram for the System  $Al_2O_3-SiO_2$ ," *J. Am. Ceram. Soc.*, 45 [5] 229-42 (1962).
  17. G. V. Kidson, "Some Aspects of the Growth of Diffusion Layers in Binary Systems," *J. Nucl. Mat.*, 3 [1] 21-29 (1961).
  18. N. L. Bowen and J. W. Greig, "The System  $Al_2O_3-SiO_2$ ," *J. Am. Ceram. Soc.* 7 [4] 242 (1924).
  19. W. D. Kingery, *Introduction to Ceramics*; p. 349. John Wiley and Sons, Inc., New and London, 1960.

20. W. Jost, Diffusion in Solids, Liquids, and Gases, Vol. I, 3rd printing (with Addendum), Academic Press, Inc., New York, 1960.
21. J. Crank, Mathematics of Diffusion, Clarendon Press, Oxford, 1956.
22. P. G. Shewmon, Diffusion in Solids, McGraw-Hill, New York, 1963.
23. M. L. Huggins and K. Sun, "Calculation of Density and Optical Constants of a Glass from Its Composition in Weight Percentage," J. Am. Ceram. Soc., 26 [1] 4-11 (1943).
24. J. Z. Frazier, R. W. Fitzgerald, and A. M. Reid, "Computer Programs EMX and EMX2 for Electron Microprobe Data Processing," Scripps Institution of Oceanography, University of California at San Diego, La Jolla, Calif., unpublished.
25. C. Matano, "The Relation Between the Diffusion Coefficients and Concentrations of Solid Metals (the Nickel-Copper System)," Jap. J. Phys., 8 [3] 109-13 (1933).
26. L. Boltzmann, "Integration of Diffusion Equations by Variable Coefficients," Ann. Physik., 53 959-64 (1894).
27. M. Appel, private communication, 1968.
28. J. O. Isard, "Electrical Conduction in the Aluminosilicate Glasses," J. Soc. Glass Tech. 43, 113T-23T (1959).
29. D. E. Day and G. E. Rindone, "Properties of Soda Aluminosilicate Glasses: I, Refractive Index, Density, Molar Refractivity, and Infrared Absorption Spectra," J. Am. Ceram. Soc., 45 [10] 489-96 (1962); "II, Internal Friction," *ibid.*, 496-504; "III, Coordination of Aluminum Ions," *ibid.*, [12] 579-81.
30. E. F. Reibling, "Structure of Sodium Aluminosilicate Melts Containing at least 50 mole % SiO<sub>2</sub> at 1500°C," J. Chem. Phys., 44 [8] 2857-65 (1966).

31. E. D. Lacy, "Aluminum in Glasses and Melts," *Phys. and Chem. of Glasses*, 4 [6] 234-38 (1963).
32. F. J. MacDowell and G. H. Beall, "Immiscibility and Crystallization in  $\text{Al}_2\text{O}_3$ - $\text{SiO}_2$  Glasses," *J. Am. Ceram. Soc.*, 52 [1] 17-25 (1969).
33. R. Rossin, J. Bersan, and G. Urbain, "Viscosity of Fused Silica and Slags Belonging to the  $\text{SiO}_2$ - $\text{Al}_2\text{O}_3$  System," *Comptes Rendus* 258 562-64 (1964).
34. T. B. King and P. J. Koros, pp. 80-85 in *Kinetics of High Temperature Processes*, edited by W. D. Kingery, John Wiley and Sons and Technological Press, New York, 1959.
35. H. Towers and J. Chipman, "Diffusion of Calcium and Silicon in a Lime-Alumina-Silica Slag," *Trans. AIME*, 203 [6] 769-73 (1955).
36. J. O'M. Bockris, J. A. Kitchener, S. Ignatowicz, and J. W. Tomlinson, "Electric Conductance in Liquid Silicates," *Trans. Faraday Soc.* 48, 75-91 (1952).
37. L. Reed and L. R. Barrett, "The Slagging of Refractories: II, The Kinetics of Corrosion," *Trans. Brit. Ceram. Soc.*, 63 [10] 509-34 (1964).

Table I. Experimental conditions and data for diffusion runs

| Sample Designation | Temp. (°C) | Time (Sec. X10 <sup>-3</sup> ) | Interface Conc. C <sub>I</sub> - (g/cc Al) | Interface Conc. C <sub>I</sub> - (wt% Al <sub>2</sub> O <sub>3</sub> ) | Mullite Growth (Microns) | D <sub>v</sub> (C) (cm <sup>2</sup> /sec)       |
|--------------------|------------|--------------------------------|--|--|--------------------------|---|
| 206 H†             | 1550       | 1209.6                         | .0863                                      | 7.2  |                          |   |
| 210 H†             | 1550       | 1382.4                         |  |  |                          |   |
| 205 H†             | 1580       | 691.2                          | .0891                                      | 7.4  |                          |   |
| 209 H†             | 1580       | 1209.6                         |  |  |                          |   |
| 026 H              | 1650       | 604.8                          | .112                                       | 9.3  | 1.24                     | 6.60 x 10 <sup>-13</sup> e <sup>30.49[Al]</sup> |
| 126 H*             | 1650       | 604.8                          |  |  |                          |   |
| 526 A              | 1650       | 604.8                          |  |  |                          |   |
| 626 A*             | 1650       | 604.8                          |  |  |                          |   |
| 027 H              | 1650       | 777.6                          |  |  |                          |   |
| 127 H*             | 1650       | 777.6                          |  |  |                          |   |
| 527 A              | 1650       | 777.6                          |  |  |                          |   |
| 627 A*             | 1650       | 777.6                          |  |  |                          |   |
| 028 H              | 1650       | 950.4                          |  |  |                          |   |
| 128 H*             | 1650       | 950.4                          |  |  |                          |   |
| 528 H              | 1650       | 950.4                          | 1.56                                       |  |                          |   |
| 628 H*             | 1650       | 950.4                          |  |  |                          |   |
| 029 H              | 1700       | 345.6                          | .155                                       | 12.9   | 3.60                     | 6.61 x 10 <sup>-12</sup> e <sup>23.96[Al]</sup> |
| 030 H              | 1700       | 604.8                          |  |  |                          |   |
| 031 H              | 1700       | 777.6                          |  |  |                          |   |
| 032 H              | 1700       | 950.4                          |  |  |                          |   |
| 033 H              | 1750       | 172.8                          | .285                                       | 22.8   | 4.71                     | 7.12 x 10 <sup>-11</sup> e <sup>17.17[Al]</sup> |
| 034 H              | 1750       | 259.2                          |  |  |                          |   |
| 035 H              | 1750       | 345.6                          |  |  |                          |   |
| 039 H              | 1800       | 14.4                           | .566                                       | 42.2   |                          | 5.31 x 10 <sup>-10</sup> e <sup>11.17[Al]</sup> |
| 040 H              | 1800       | 21.6                           |  |  |                          |   |
| 041 H              | 1800       | 28.8                           |  |  |                          |   |

\* - Mullite-fused SiO<sub>2</sub> couples  
 † - Cristobalite-sapphire couples  
 All others - sapphire-fused silica couples

H - Helium  
 A - Argon



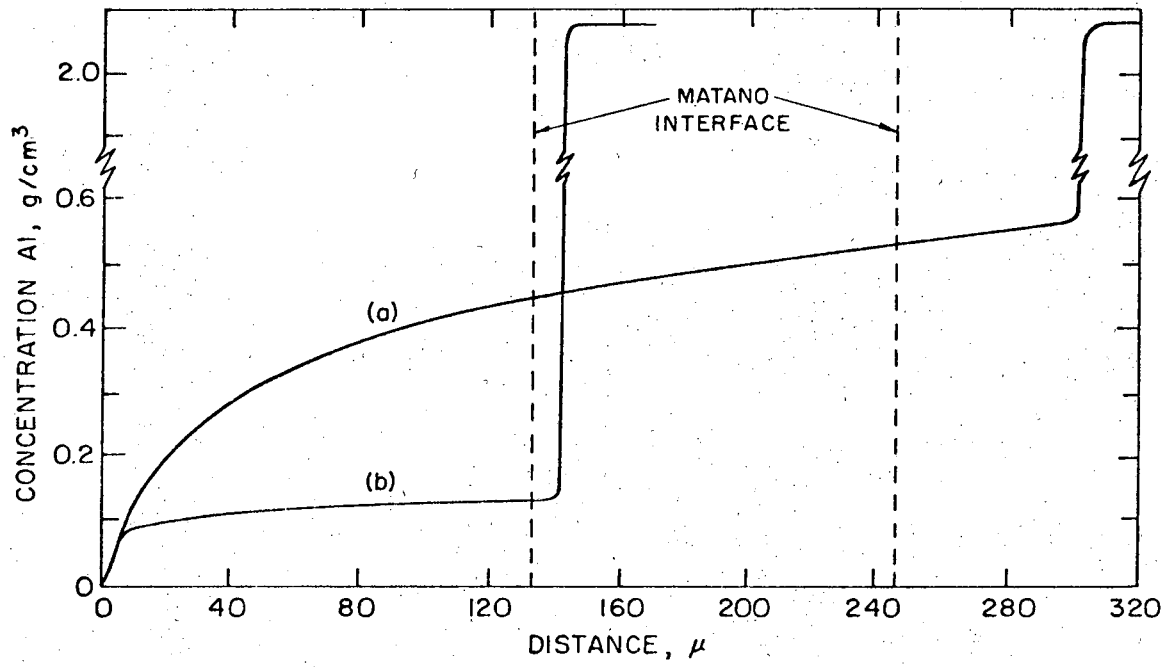
Table II. Diffusivity data for the  $\text{Al}_2\text{O}_3$ - $\text{SiO}_2$  system

| $C_{\text{Al}^{+3}}$ ( $\text{gm}/\text{cm}^3$ ) | $C_{\text{Al}_2\text{O}_3}$ (wt%) | $D_0$ ( $\text{cm}^2/\text{sec}$ ) | $Q$ (Kcal/mole) |
|--|-----------------------------------|------------------------------------|-----------------|
| .05  | 4.30                              | $3.47 \times 10^{23}$              | $307.5 \pm 1.0$ |
| .07  | 5.96                              | $2.43 \times 10^{21}$              | $286.2 \pm 1.0$ |
| .09  | 7.60                              | $1.64 \times 10^{19}$              | $264.8 \pm 0.4$ |
| .11  | 9.24                              | $1.66 \times 10^{17}$              | $245.0 \pm 0.3$ |
| .15  | 12.40                             | $9.93 \times 10^{12}$              | $203.3 \pm 0.4$ |
| .20  | 16.40                             | $6.29 \times 10^7$                 | $151.9 \pm 0.5$ |
| .25  | 20.10                             | $3.38 \times 10^2$                 | $99.9 \pm 0.6$  |
| .28  | 22.30                             | $1.91 \times 10^{-2}$              | $58.6 \pm 0.8$  |

## Figure Captions

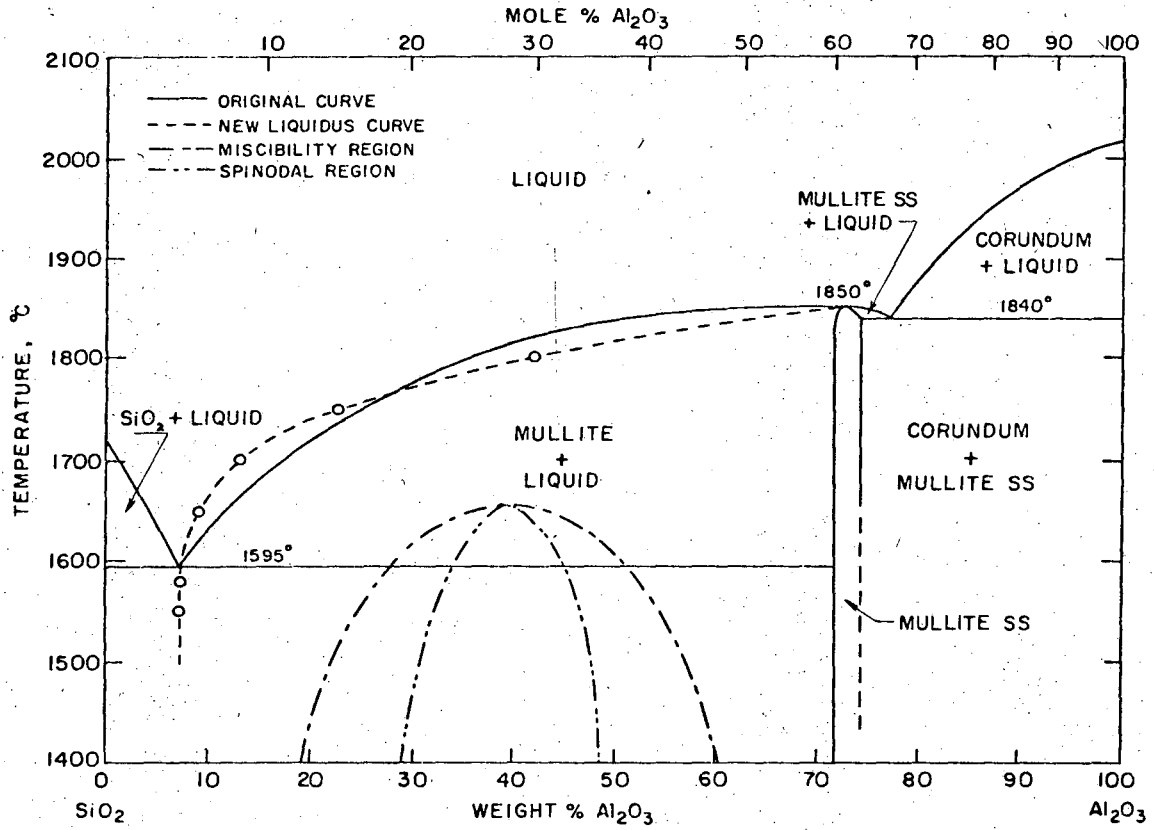
- Fig. 1. Concentration of aluminum ion vs. distance for sapphire-fused silica couples heated in He at (a) 1800°C for 4 h and (b) 1650°C for 11 days.
- Fig. 2. New mullite liquidus curve (dash line) superimposed on the  $\text{Al}_2\text{O}_3$ - $\text{SiO}_2$  diagram determined by Aramaki and Roy.<sup>16</sup> Region of liquid immiscibility as determined by MacDowell and Beal<sup>32</sup> is also shown.
- Fig. 3. Microstructure of the diffusion zone formed between cristobalite (top) and sapphire (bottom) annealed at 1580°C for 8 days. The amorphous phase is shown at the interface. The worm-like features are cracks filled with the mounting resin.
- Fig. 4. Single eutectic metastable phase diagram proposed to explain glass formation at subsolidus temperatures in the  $\text{Al}_2\text{O}_3$ - $\text{SiO}_2$  system.
- Fig. 5. Microstructure of the diffusion zones formed between alumina and silica (a) 1650°C, 7 days; (b) 1700°C, 4 days; (c) 1750°C, 4 days; (d) 1800°C, 6 h. Position of phases is the same as Fig. 3 with the addition of a thin layer of interfacial mullite in (a), (b) and (c) and crystallization of mullite in diffusion zone on cooling in (b), (c) and (d).
- Fig. 6. Plots of thickness of mullite growth in  $\text{Al}_2\text{O}_3$ - $\text{SiO}_2$  diffusion couples vs. square root of time for 1650, 1700 and 1750°C. Broken lines represent constant times.
- Fig. 7. Graph of thickness of mullite for various times vs. temperature.

- Fig. 8. Comparison of measured and calculated densities for aluminosilicate glasses using factors of Huggins and Sun.<sup>23</sup>
- Fig. 9. Semi-log plot of computer determined diffusivities vs. concentration for  $\text{Al}_2\text{O}_3\text{-SiO}_2$  at 1800°C for 4 h in He.
- Fig. 10. Log diffusivity vs. reciprocal of absolute temperature at constant  $\text{Al}^{+3}$  concentrations.



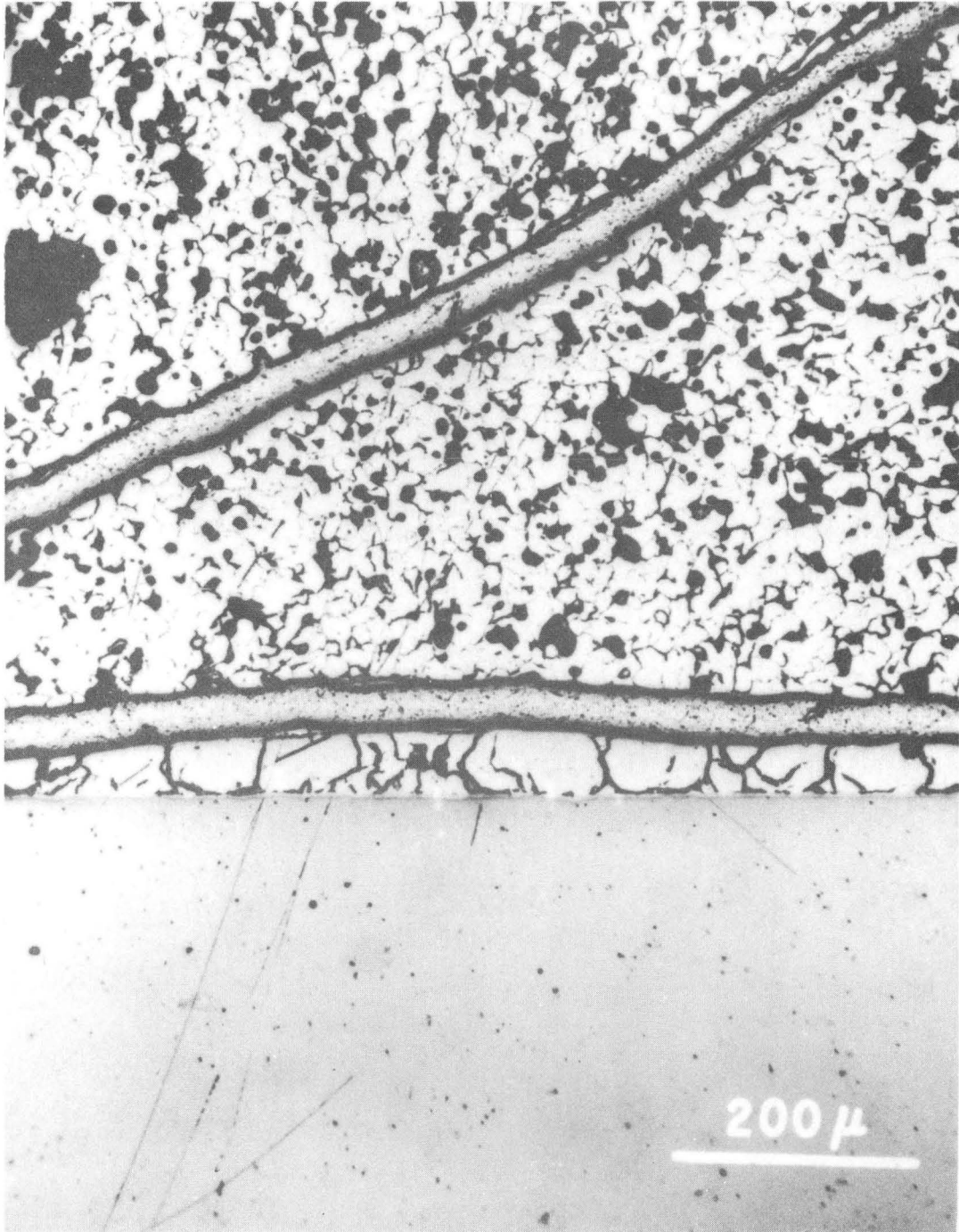
XBL714-6659

Fig. 1



XBL 707-1417

Fig. 2



XBB 707-3035

Fig. 3

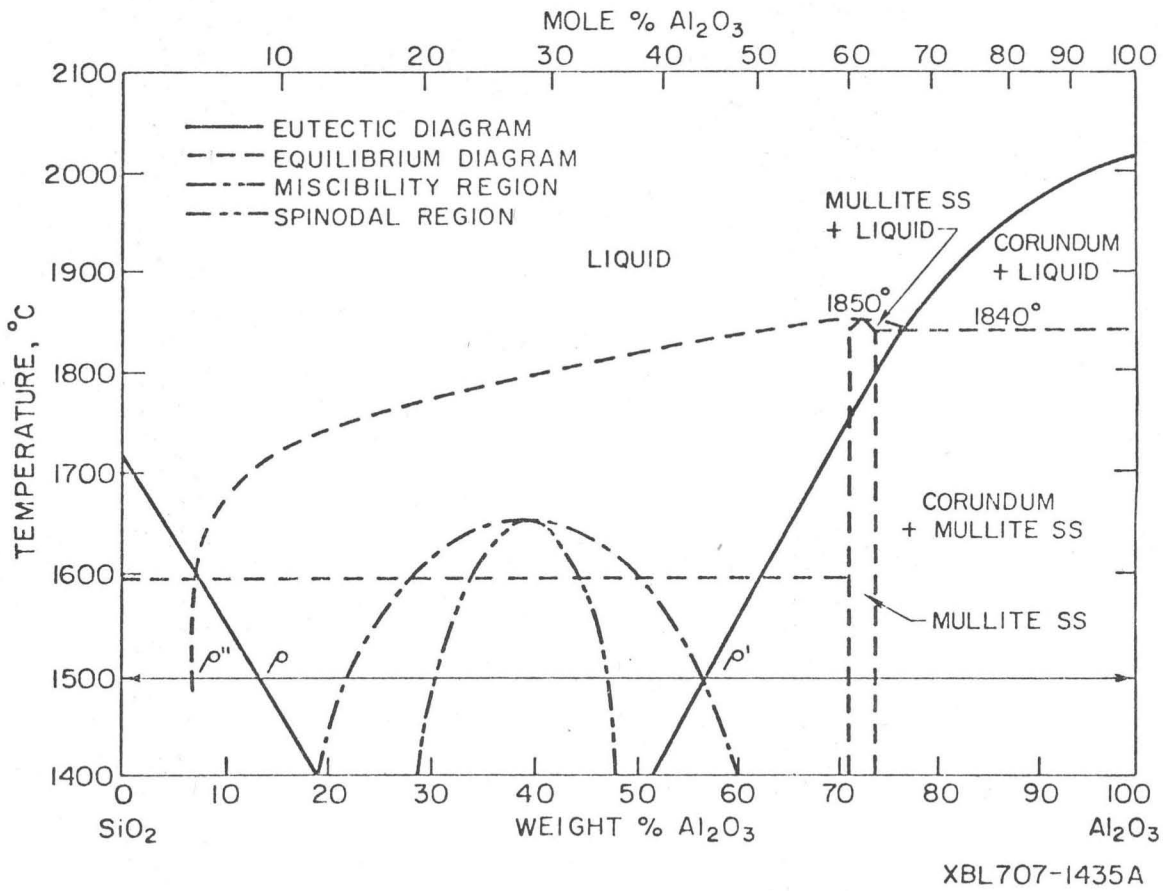
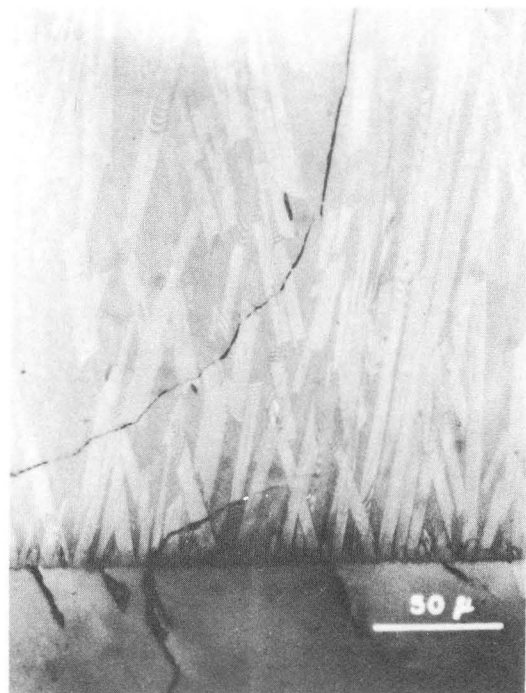
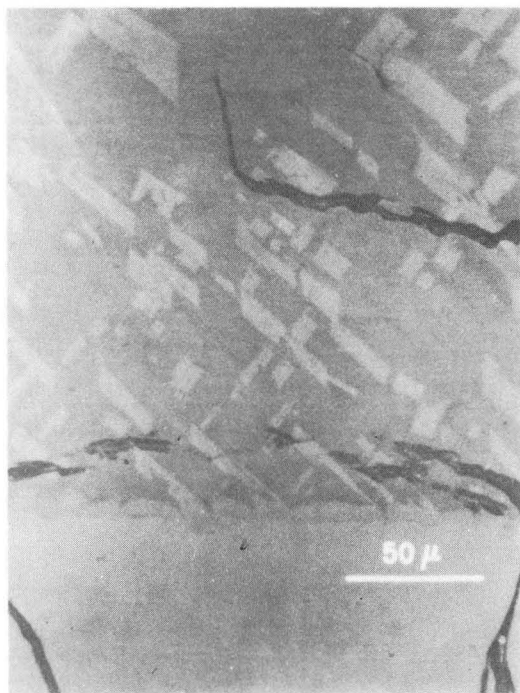
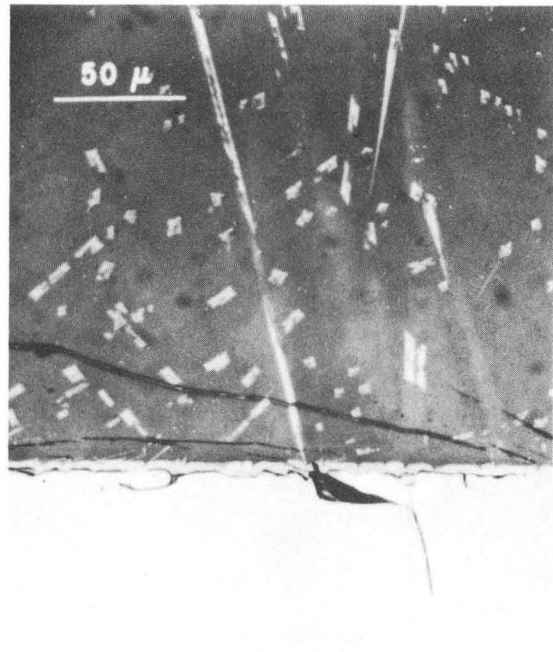
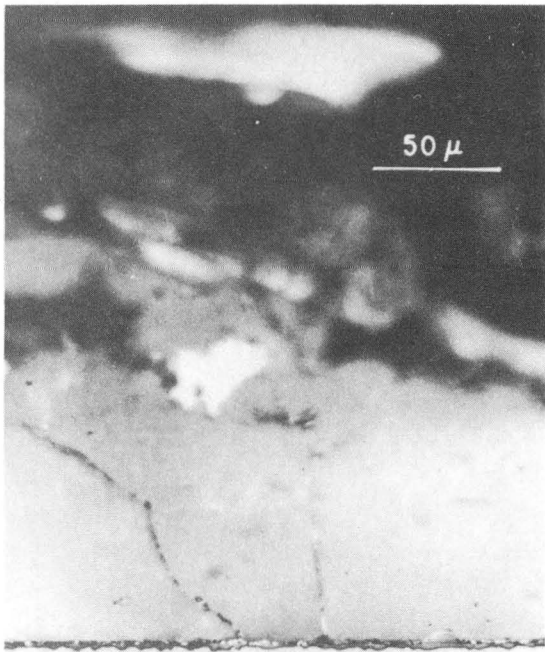


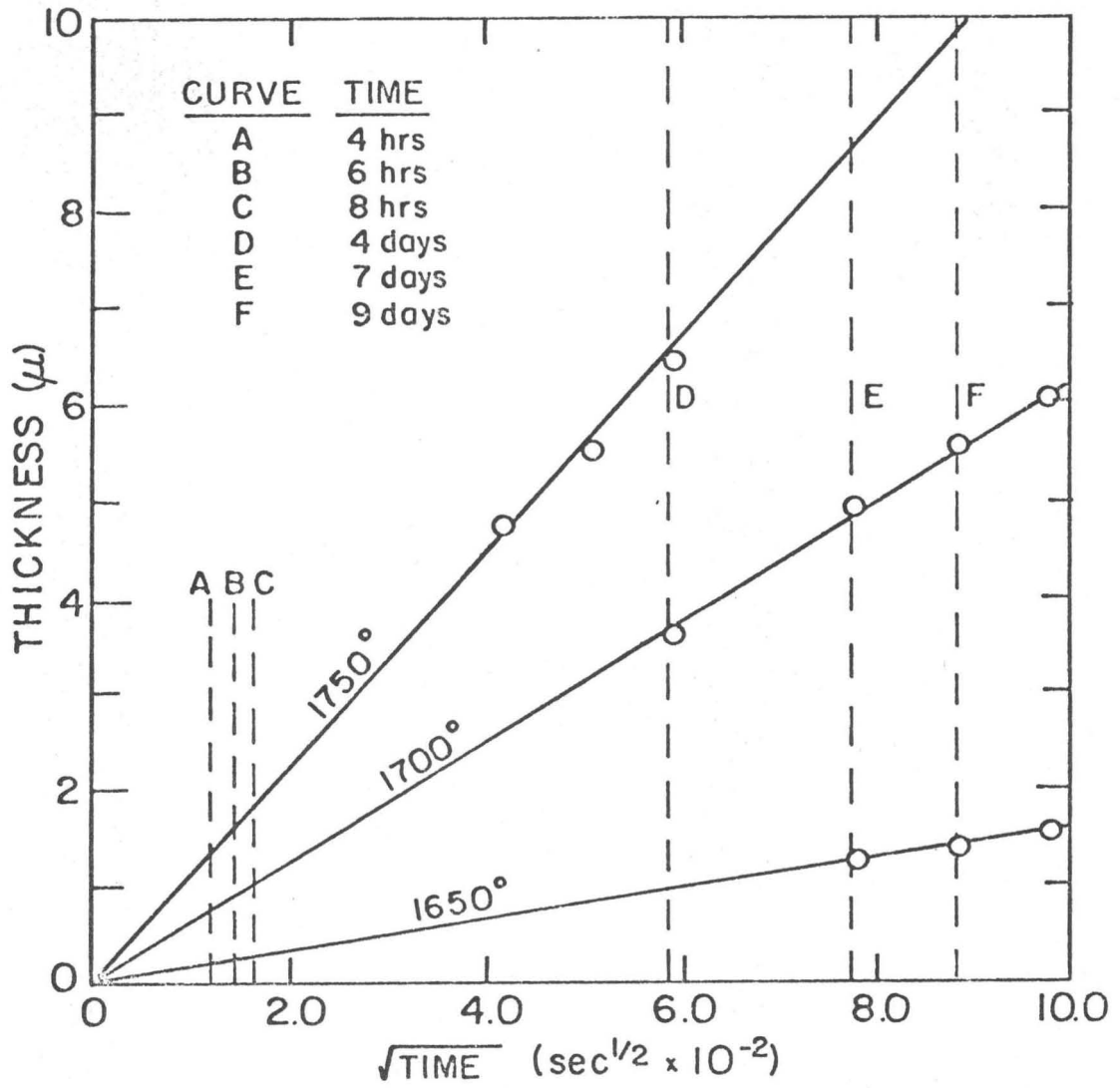
Fig. 4



XBB 714-1529

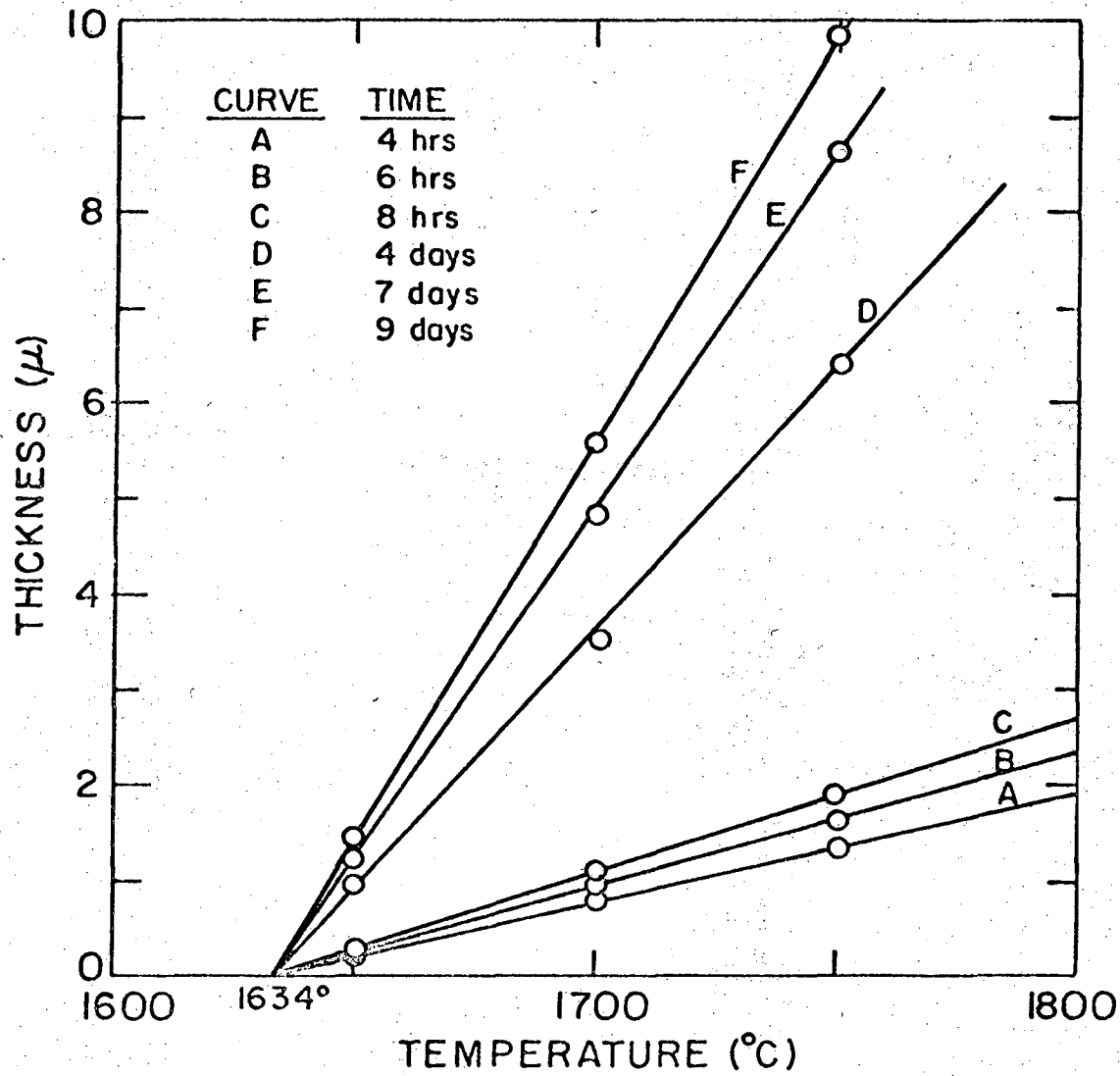
Fig. 5





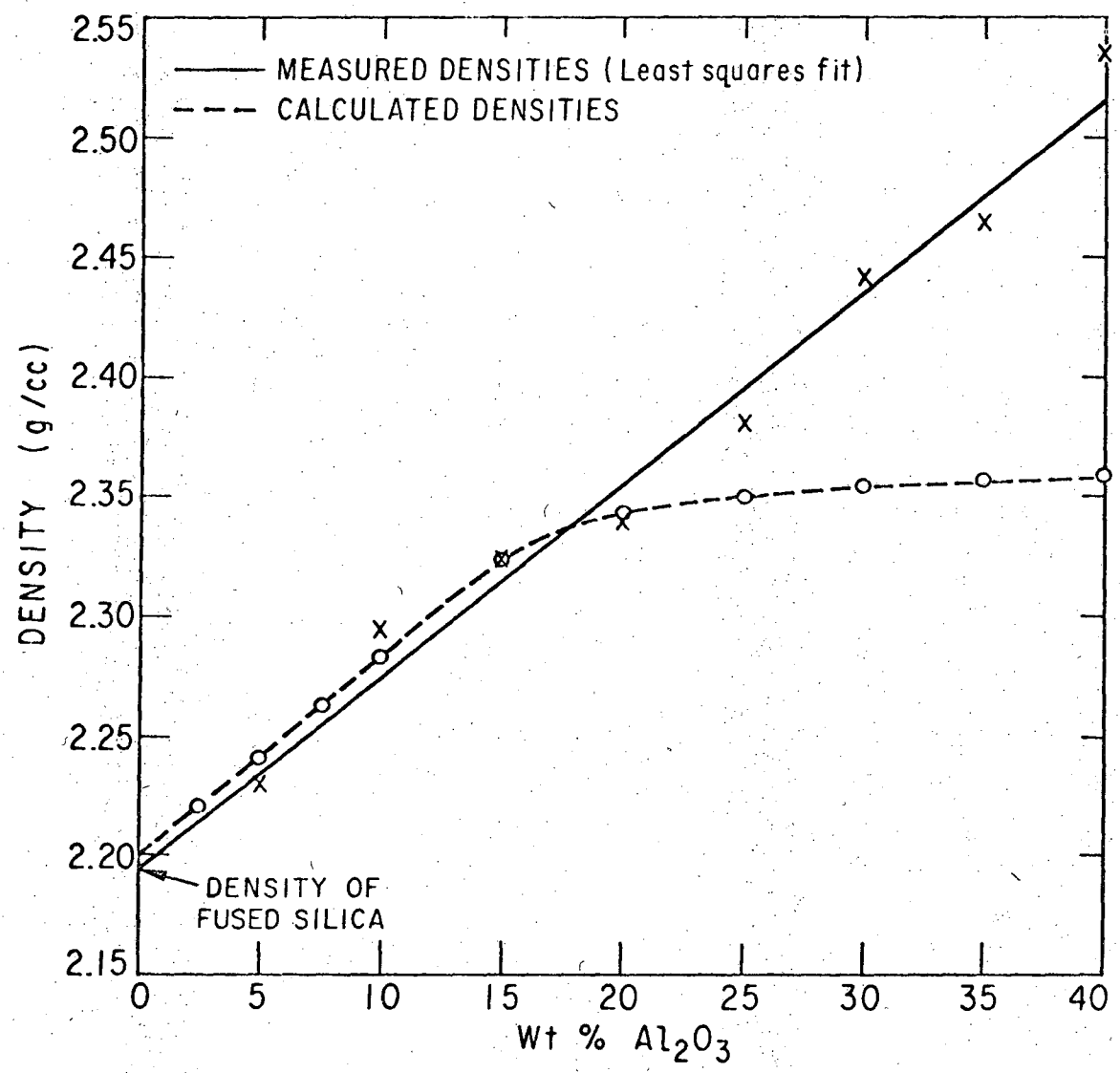
XBL 707-1418

Fig. 6



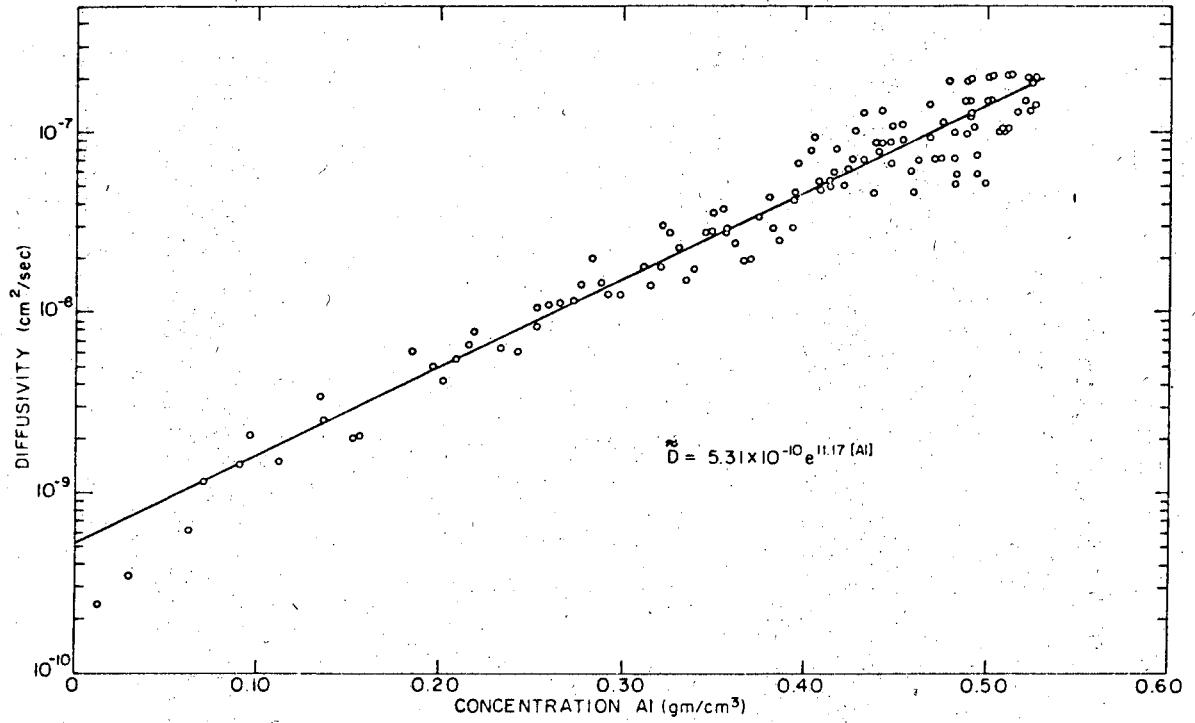
XBL 707-1419

Fig. 7



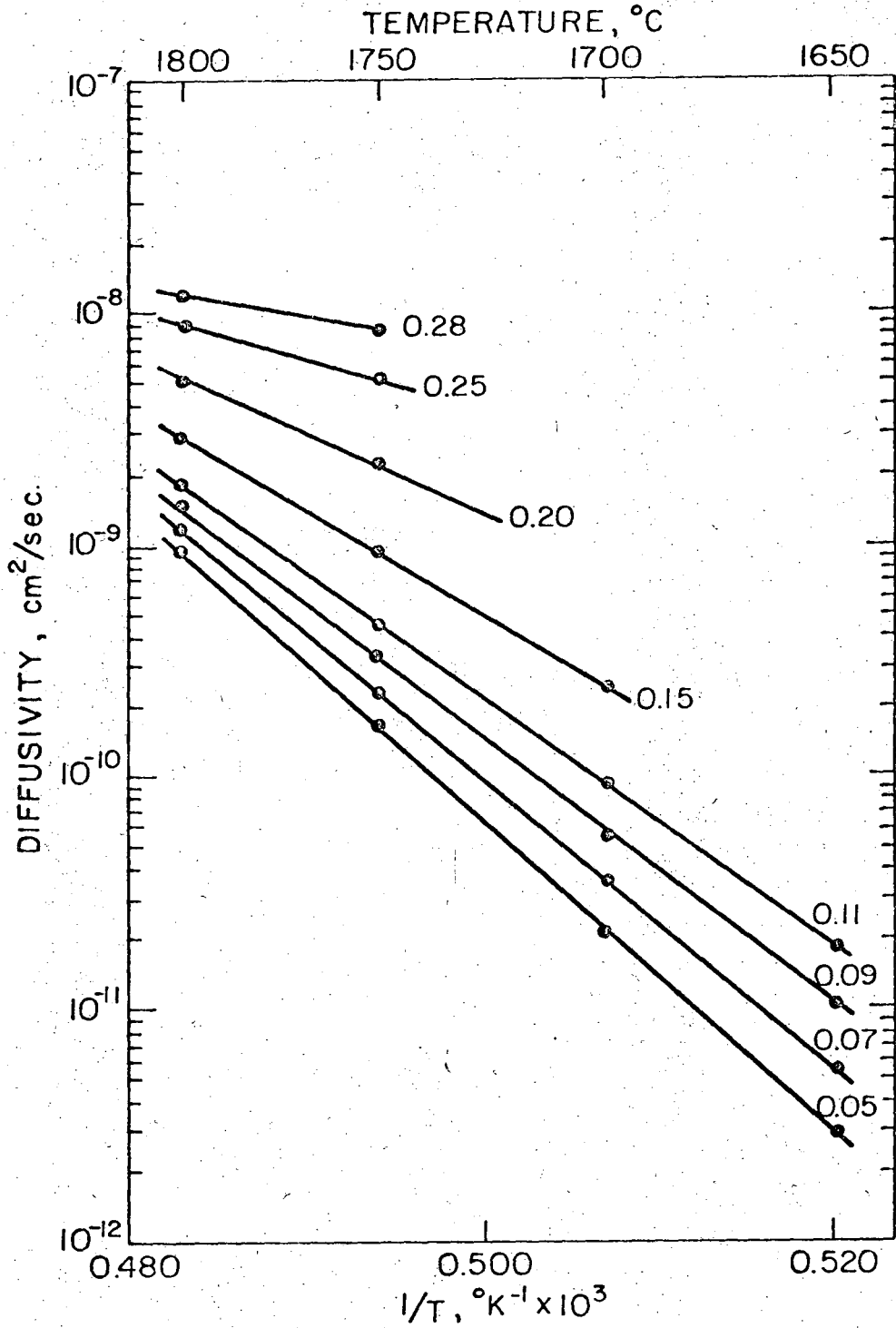
XBL 707-1408

Fig. 8



XBL 707-1430

Fig. 9



XBL707-1431A

Fig. 10

LEGAL NOTICE

*This report was prepared as an account of work sponsored by the United States Government. Neither the United States nor the United States Atomic Energy Commission, nor any of their employees, nor any of their contractors, subcontractors, or their employees, makes any warranty, express or implied, or assumes any legal liability or responsibility for the accuracy, completeness or usefulness of any information, apparatus, product or process disclosed, or represents that its use would not infringe privately owned rights.*

TECHNICAL INFORMATION DIVISION  
LAWRENCE BERKELEY LABORATORY  
UNIVERSITY OF CALIFORNIA  
BERKELEY, CALIFORNIA 94720